

Accepted Manuscript

Modified diatomites for Fenton-like oxidation of phenol

N. Inchaurreondo, C.P. Ramos, G. Žerjav, J. Font, A. Pintar, P. Haure

PII: S1387-1811(16)30489-9

DOI: [10.1016/j.micromeso.2016.10.026](https://doi.org/10.1016/j.micromeso.2016.10.026)

Reference: MICMAT 7966

To appear in: *Microporous and Mesoporous Materials*

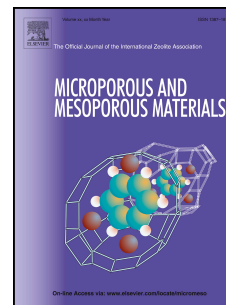
Received Date: 8 August 2016

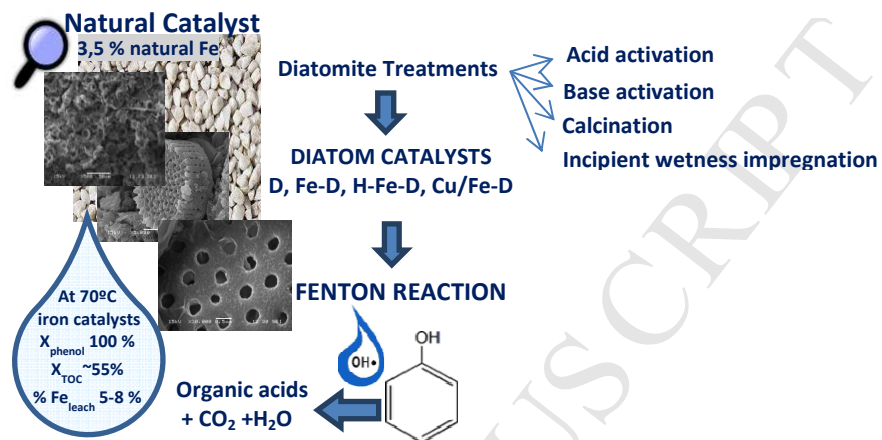
Revised Date: 21 September 2016

Accepted Date: 18 October 2016

Please cite this article as: N. Inchaurreondo, C.P. Ramos, G. Žerjav, J. Font, A. Pintar, P. Haure, Modified diatomites for Fenton-like oxidation of phenol, *Microporous and Mesoporous Materials* (2016), doi: 10.1016/j.micromeso.2016.10.026.

This is a PDF file of an unedited manuscript that has been accepted for publication. As a service to our customers we are providing this early version of the manuscript. The manuscript will undergo copyediting, typesetting, and review of the resulting proof before it is published in its final form. Please note that during the production process errors may be discovered which could affect the content, and all legal disclaimers that apply to the journal pertain.





Modified diatomites for Fenton-like oxidation of phenol

N. Inchaurreondo^{a,*}, C.P. Ramos^b, G. Žerjav^c, J. Font^d, A. Pintar^c, P. Haure^a

^aDpto. de Ingeniería Química/Div. Catalizadores y Superficies-INTEMA-

CONICET/Universidad Nacional de Mar del Plata, Mar del Plata 7600, Argentina

^bDepartamento de Física de la Materia Condensada, GiyA-CAC-CNEA, Av. Gral. Paz 1499

San Martín, Buenos Aires, Argentina

^cDepartment for Environmental Sciences and Engineering, National Institute of Chemistry,

Hajdrihova 19, SI-1001 Ljubljana, Slovenia

^dDepartament d'Enginyeria Química, Escola Tècnica Superior d'Enginyeria Química,

Universitat Rovira i Virgili, Tarragona, 43007 Catalonia, Spain

*E-mail address: ninchaurreondo@gmail.com

*Tel./Fax: +542234816600-242/+542234810046

Abstract - Raw diatomites were modified by acid or base treatments; addition of Fe or Cu species through the incipient wet impregnation method (IWI) and calcination at 700°C. Samples were characterized by X-ray powder diffraction (XRD), scanning electron microscopy (SEM-EDX), Mossbauer spectroscopy, point of zero charge (PZC), pyridine temperature programme desorption (TPD), thermogravimetric analysis (TGA) and BET surface area determination.

According to characterization results, four samples were selected: simply calcined Diatom (D), iron added (Fe-D), acid treated Fe reimpregnated (H-Fe-D) and copper added (Cu/Fe-D). Materials were tested as catalysts for the peroxidation of phenol solutions (1000 mg/L) in a batch laboratory reactor, at different operating conditions in 5 hours tests. D, Fe-D and H-Fe-

D samples allowed complete phenol removal under all the operating range studied. At optimum conditions, TOC conversions of 50-55 % were obtained. Metal ions added through the IWI procedure resulted more labile than metal present originally. The acidic treatment favoured the initiation of the reaction showing a reduction of the induction period at almost neutral initial pH. The Fe-D catalyst exhibited poor performance, lower reactions rates and higher Fe leaching. Conversely, high TOC conversions (80 %) were achieved with Cu/Fe-D, however, Cu leaching was excessive (12.7 %). D and H-Fe-D samples were used in consecutive runs (up to 20 h) maintaining phenol conversion and TOC reduction. Overall, a good performance was obtained, even comparable to more sophisticated Fe catalysts.

Keywords: diatomites, phenol, natural catalyst, Fenton-like

1. Introduction

Advanced oxidation processes (AOPs) for environmental requirements are characterized by the rapid and non-selective oxidation of organic matter by the action of hydroxyl radicals. Among AOPs, the heterogeneous Fenton reaction for the degradation of organic pollutants has been thoughtfully studied [1-2]. In particular, the Fenton-like reaction of model phenol solutions over Fe based catalyst has received considerable attention, as shown in Table 1. This compound is relatively detrimental in terms of catalyst stability, since higher concentrations are used and the pH reaches low values during the oxidation process. Moreover, a high concentration of complexing reaction intermediates is generated promoting the lixiviation of the active phase. Accordingly, the search for an active, selective, stable and low cost catalyst constitutes one of the main targets towards the industrial implementation of Fenton related AOP.

Following the green chemistry principles, several recent studies have proposed the use of natural materials as catalysts [11-13]. In particular, Inchaurredo et. al. [13] tested natural

diatomites with a simple thermal treatment for the oxidation of an azo-compound, Orange II. Diatomites are extremely cheap, ecofriendly materials, highly available worldwide. They have porous structure, low density, and relatively high surface area and iron content. Results obtained with diatomites were comparable to those obtained using more sophisticated and expensive catalyst systems. However, the thermal treatment significantly decreased diatomite surface area. This effect could be compensated by acid or base treatments. Acid treatment may increase surface area and pore size, due to the elimination of impurities responsible of pore blockage [14-15]. In the presence of water, oxides on the surface of diatomite are covered with hydroxyl groups which behave as Brönsted acid sites. The treatment with acid would increase the surface area and the concentration of these medium acid sites [15].

On the other hand, the alkaline treatment could lead to the formation of soluble silicates SiO_3^{2-} resulting in the creation of pores, flaws, cracks and an increased surface area [16-18].

As seen in Table 1, Fe-based catalysts are mostly efficient at a narrow pH range in which no induction period is detected. Therefore, bimetallic Fe-Cu catalysts are receiving considerable attention for Fenton-like processes since copper is active in a wider pH range and allows higher mineralization [19-20].

The present contribution carefully assesses the impact of acid or base treatments and Fe or Cu impregnation procedures on diatomite samples. Pretreatments modify several properties such as surface area, pore size distribution, acid sites, point of zero charge, metal active sites dispersion, surface morphology, etc., which in turn determine catalytic performance.

Selected samples were used in the Fenton-like oxidation of concentrated aqueous phenol solutions at various operating conditions. Intermediate products adsorption was addressed. Leaching and resulting homogeneous contribution were also studied to evaluate catalyst stability and to determine the nature of the oxidation process.

2. Experimental

2.1. Samples preparation

2.1.1. Raw sample preliminary treatment

The diatomite sample was purchased from a local supplier (Marysol), harvested from a deposit located in Ing. Jacobacci, Río Negro, Argentina. The raw diatomite (sample without any previous treatment) was sieved and the fraction of 7-8 mesh (2.38-2.83 mm) was collected.

2.1.2. Acid activation

Diatomite samples were treated with HNO_3 (65 % wt) at 70°C for 3 hours under reflux (sample Raw- HNO_3), since the use of HNO_3 at low temperature reduces the dissolution of iron in contrast to HCl or H_2SO_4 [21].

2.1.3. Base activation

In this case the raw sample was treated with NaOH (1 mol/L) for 30 min at room temperature in order to avoid drastic dissolution of the sample.

2.1.4. Incipient wetness impregnation

The impregnation was performed before calcination since the thermal treatment reduces the concentration of hydroxyl groups, which has a detrimental effect on adsorption [22].

The diatomite support was dried at 120°C overnight. Then, the required amount of an aqueous solution of $\text{Fe}(\text{NO}_3)_3 \cdot 9\text{H}_2\text{O}$ (Appli Chem, analytical-reagent grade) or $\text{Cu}(\text{NO}_3)_2 \cdot 2\frac{1}{2}\text{H}_2\text{O}$ (p.a., Riedel-de Haën, Germany, analytical-reagent grade) was slowly added to the support at room temperature. This amount was calculated by using the water pore volume of the support. The concentration of the solution was adjusted to obtain 2 % wt loading, in two cycles of impregnation. Samples were dried at room temperature overnight, 24 hours at 120°C and then calcined at 700°C under air atmosphere for 4 hours.

Five samples were obtained, respectively named: (i) D (sample calcined at 700°C, not impregnated), (ii) Fe-D (impregnation performed on raw diatomite), (iii) H-Fe-D (impregnation performed on the acid activated diatomite), (iv) Na-Fe-D (impregnation performed on the base activated diatomite) and (v) Cu/Fe-D (Cu impregnation of the raw sample, keeping the natural iron present in the diatomite).

2.1.5. Frustules and clays

To disclose the nature of catalytic sites, the separation of frustules from clay was attempted, following the method proposed by Pedersen et al. [23]. The sample was crushed, suspended into distilled water and treated with ultrasonication for 15 min. The sample was left for 20 min to allow the frustules to settle, whereas the clay sized particles remained in suspension. The suspended clay was removed by decantation and the diatom frustules resuspended. This was repeated three times for each extraction of frustules.

2.2. Catalyst characterization

The Fe content was determined using a commercial kit (FeVer 2™, Hach), after digestion of samples with HF (70 % wt).

Specific surface area was determined by N₂ adsorption/desorption at -196°C (Micromeritics, model TriStar II 3020). Prior to measurements, degassing of samples was conducted under a N₂ stream (Linde, purity 6.0) with programmed bi-level heating, starting with the first heating stage at 90°C for 60 min and followed by the second heating stage at 180°C for 240 min. The specific surface area of materials was calculated by means of BET theory. Pore size distribution was calculated from the desorption branch of the corresponding nitrogen isotherms, employing the BJH method.

Powder X-ray diffraction (XRD) patterns of the samples were obtained with a D5000 diffractometer (Siemens) employing CuK α radiation. The analysis was carried out at 40 kV

and 30 mA. The diffractograms were recorded over $5^\circ < 2\theta < 75^\circ$ angles, and compared to the X-ray powder files to confirm phase identities.

The surface morphology was investigated by means of a scanning electron microscope JEOL JSM-6460LV. The elemental composition was determined by energy dispersive X-ray spectroscopy (EDS) using an EDAX Genesis XM4-Sys60 equipment.

Mössbauer spectra were obtained at room temperature (RT) with a conventional constant acceleration spectrometer in transmission geometry with a $^{57}\text{Co}/\text{Rh}$ source. Measurements were recorded at 10 mm/s and then fitted using the Normos program developed by Brand, 1987. Isomer shift values are listed relative to that of $\alpha\text{-Fe}$ at RT.

The point of zero charge (PZC), was determined by means of mass titration method, as reported by Preočanin and Kallay [24]. Portions of diatomites (0.05 g) were added to a stirred aqueous solution with initial pH=6. The pH of the system changes gradually and approaches to a constant value, which equals to PZC. Measurements were performed at 25°C in 25 mL of 0.005 mol/L NaCl aqueous solutions, purged with 750 mL/min of N_2 .

Acidic properties were determined by temperature programmed desorption (TPD) analysis using Pyris 1 TGA instrument (Perkin Elmer). The samples were first heated in air to 500°C ($10^\circ\text{C}/\text{min}$, hold at final temperature for 15 min) to eliminate surface impurities. Then the samples were cooled to 120°C and purged with N_2 , followed by the surface saturation with pyridine until constant weight. The excess of probe molecule was then removed in N_2 flow (120 min). TPD of pyridine was carried out by heating samples to 800°C at $20^\circ\text{C}/\text{min}$.

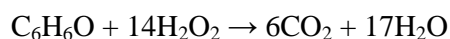
Thermogravimetric analyses (TGA Q500 V20.13) were performed using a heating rate of $20^\circ\text{C}/\text{min}$, under air atmosphere.

2.3. Oxidation tests

In a typical experiment, a known amount of fresh catalyst was put into 200 mL of 1 g/L of phenol (p.a., Cicarelli) aqueous solution under continuous stirring. When the reaction

temperature was reached, an H₂O₂ dose (Cicarelli, 30 %) of 1.3 the stoichiometric requirement was added into the system and the reaction started. Liquid-phase samples were withdrawn at different times up to 300 min, and analyzed to determine phenol, hydrogen peroxide and total organic carbon (TOC) conversions. During the reaction, pH value was monitored but not controlled. Tests were performed at 60 or 70°C.

The mineralization reaction is stated to be:



Phenol was detected and measured by UV/VIS absorbance at $\lambda=508$ nm with a standard colorimetric method [25]. Hydrogen peroxide was determined by an iodometric titration method [25], and TOC concentrations were measured using a TOC analyzer (Shimadzu, model TOC-VCPN). Values reported here represent an average of at least two measurements. Total Fe concentration leached in the supernatant was measured using a commercial kit (FeVer 2™, Hach).

3. Results and discussion

3.1. Catalyst characterization

Fresh catalyst samples (samples that have not been tested) were characterized together with selected samples used in four consecutive phenol oxidation tests (190 mmol/L of H₂O₂, 70°C, catalyst loading equivalent to 100 mg/L of Fe). Used samples were only filtered from the reaction media and dry at room temperature before being reused.

3.1.1. Fe content

The Fe content is presented in Table 2 with a 0.5 standard deviation value. The obtained data are in agreement with the values obtained by SEM-EDX examination.

3.1.2. BET surface area and pore size distribution

The values of BET surface area are listed in Table 2. N₂ adsorption-desorption isotherms are presented in Figs. 1 and 2. The calcination generates the sintering of the material which

contributes to the reduction of BET surface area.

Contrary to the results obtained by Tsai et al. [16] and Jian et al. [17], the base treatment caused a decrease of BET surface area and pore volume. Additionally, the SEM-EDX results showed an increase of the Na surface content (see Table S1), probably present as a sodium silicate layer formed during the dissolution process, which caused the reduction of the surface area [26].

The acid treatment increased BET surface area (20 %) due to the elimination of impurities responsible of pore blockage. The pore distribution shows an increment of the percentage of mesopores at around 10 nm and a slight reduction of the proportion of micropores (<2 nm) (Fig. 3).

The impregnation and calcination procedures generated a reduction of BET surface area, specially in the case of the Fe-D sample. The acid treatment compensated such drastic decrease. The impregnation with Cu did not significantly affect BET surface area.

Used D and H-Fe-D samples showed an increase of BET surface area and a slight increase of total pore volume. Pore distribution (Fig. 4) shows a higher proportion of pores of 2-3 nm. These pores would emerge as the result of the elimination of some impurities due to the acidic and oxidizing conditions achieved during the reaction.

3.1.3. SEM-EDX analysis

The chemical weight composition of diatomite reveals the presence of oxides of Si and Al together with other mineral impurities, i.e. Fe, Na, Ca, Mg, etc. (Table S1).

Cu seems to be homogeneously dispersed in the Cu/Fe-D sample. However, some diatomite particles show dark spots noticeable to the naked eye. Clusters of CuO where the percentage of Cu increases up to 30 % wt/wt were identified (Fig.S1).

Calcium is removed by both base and acid treatments (dissolution of CaCO_3). There are no differences in the content of C, Si, Mg, O or Al (Table S1). The surface of the catalyst treated with NaOH presents several cracks, which are related to its observed fragility (Fig. 5b).

The morphology of the H-Fe-D and Fe-D samples is similar to the morphology of the raw sample; no clusters of iron oxide were identified (Fig. 5a, c and d). Fe seems to be homogeneously dispersed in the impregnated samples and no differences between fresh and used samples were detected.

The clay fraction extracted from diatomite presented a smoother surface and smaller particles (Fig. S2). However, the SEM-EDX composition of both samples is quite similar (Table S2) to the SEM-EDX results obtained from the raw diatomite sample. However, one can distinguish the presence of frustules in the clay sample, suggesting incomplete separation of the phases.

3.1.4. Mössbauer spectroscopy

For the sake of clarity in the subsequent discussion, the room temperature Mössbauer spectra of the examined samples are shown in two different groups in Fig. 6. Fig. 6a displays the raw material, the clay and the frustule spectra, while Fig. 6b exhibits the spectra of D, H-Fe-D and Fe-D samples. The corresponding hyperfine parameters are displayed in the supplementary material Table S3.

The raw material sample was fitted to two overlapping doublets reflecting that all the iron in the sample is present as Fe^{3+} . The major doublet (D1) is typical of Fe^{3+} in *cis* octahedral (M2) sites of smectites and related minerals [27-31]. The octahedral Fe seems to be in an environment somewhat similar to that of nontronite (iron-rich end member of the smectite group), which is normally *trans* vacant [32-33]. The minor doublet (D2) is consistent with some tetrahedral Fe^{3+} .

The clay spectrum shows that almost all iron is present as Fe^{3+} in *cis* octahedral sites as in nontronite (D1), but also a small contribution of *trans* octahedral sites can be noticed (D2). No evidence of tetrahedral Fe^{3+} sites is found, in contrast to the raw sample.

Instead, the frustule sample displays a major fraction of Fe^{3+} in *cis* octahedral sites (D1), but also a minor fraction of Fe^{3+} in tetrahedral sites (D3) and a minute fraction of Fe^{2+} (D4).

It is clear that the frustule fraction in the raw diatomite is very poor, so the insignificant amount of Fe^{2+} could only be distinguished after the separation process. The clay contributes only Fe^{3+} in *cis* octahedral sites and the frustule adds Fe^{3+} in tetrahedral sites. Mössbauer spectroscopy helped to distinguish different iron sites in frustule and clay samples. Anyway, taking also into account SEM observations and XRD results it can be concluded that the separation process was not totally successful.

On the other hand, for all the samples calcined at 700°C (D, Fe-D and H-Fe-D), an increase in QS in the octahedral sites (D1) is the product of a dehydroxylation of the octahedral planes of the clay. This process releases water from the tetrahedral sheets, so the number of ligands of the octahedral iron reduces in some of the octahedrons of the clay structure. The other octahedrons slightly distort and the iron site symmetry reduces.

An additional Fe^{3+} doublet, corresponding to dehydroxylated surface sites, was found (D5) for the Fe-D and H-Fe-D samples. The only difference between samples is the fraction of dehydroxylated surface sites, greater in the HNO_3 treated material, probably due to the higher surface area. Additionally, if the impregnated iron is in the form of hematite in a few nanometers size, it could be masked in the spectrum of diatomite.

3.1.5. XRD analysis

The diffractograms of the raw material and clay are similar, pointing out the presence of albite (A), nontronite (N) and quartz (Q) as the main components (Fig S3). The only difference is that in the raw material a minor amount of iron oxide (W: wustite) is apparent.

On the contrary, the pattern for the frustule shows a major content of albite and quartz and less nontronite. Nevertheless, as mentioned above, it is clear that the separation of clay and frustule was not totally accomplished.

On the other hand, the only difference between the calcined Fe-impregnated samples (with and without HNO₃ treatment (H-Fe-D and Fe-D) seems to be in the content of quartz and albite fractions (Fig. 7)

In the Cu/Fe-D sample, CuO and a small fraction of maghemita were identified (Fig. S4).

3.1.6. Point of zero charge (PZC)

At $\text{pH} < \text{PZC}$, surface sites are protonated and the surface becomes positively charged, while at $\text{pH} > \text{PZC}$, the surface hydroxides lose their protons and the surface becomes anionic [34]. Accordingly to results presented in Fig. 8, the point of zero charge equals to 8.4 for D, 7.4 for Fe-D and 5.3 for H-Fe-D samples.

3.1.7. TPD of pyridine

Acid sites were determined and results are presented in Table 3 and Fig. 9. The samples exhibit different pyridine desorption peaks, indicating that the surface acidity varies after acid treatment and/or impregnation of the catalyst. Lower temperatures peaks correspond to weaker acid sites. The impregnation of the catalyst (Fe-D) drastically reduced the amount of acid sites and a small peak at 523°C referred to medium acid sites appeared. This peak could be related to oxide particles, which expose rather Lewis acidity. This peak is larger for the H-Fe-D sample, where iron may be more dispersed and accessible for pyridine molecules [35]. The reduced amount of acid sites in the Fe-D sample may be related to the lower BET surface area.

The acid treatment increased the amount of weak acid sites (238°C) and a large peak at 556°C related to the Lewis acidity of the Fe added appeared. The higher BET surface area of this sample may result in an increased hydroxyl group exposure to pyridine, resulting in a higher

detection of medium-acid sites [15]. The original peak at 630°C almost disappeared after impregnation and calcination. Since concentration of Lewis acid sites depend on calcination temperature and presence of clays impurities, the removal of surface impurities (Al_2O_3 , Fe_2O_3 , MgO) during acid treatment could cause the disappearance of these relatively strong acid sites [15].

Therefore, acid treatment may enhance the concentration of hydroxyl groups, but decrease the concentration of Lewis acid sites.

3.1.8 Thermogravimetric analysis

The thermogravimetric analyses were performed on the D and H-Fe-D samples used in 4 consecutive reaction tests of 5 hours each (Fig S5-S8).

An endothermic peak centered at 45.66°C was attributed to the loss of adsorbed water. The small peak around 439°C may be related to the liberation of water caused by the dehydroxylation of external silanol groups. In the high temperature region, the endothermic peak at 860°C could be associated to siloxane bridges resulting from dehydroxylation of isolated silanol groups on the internal surface of diatomite [21].

The shoulder at 100°C could be related to organics intermediates adsorbed during reaction as they are only noticeable in the used samples. There is no significant difference between the weight loss of fresh and used samples.

3.1.9. Diatomite stability studies

To assess the effect of pH on catalysts stability, a series of tests was performed at room temperature by contacting a catalyst loading equivalent to 100 mg/L of Fe or Cu with 200 mL of bidistilled water at pH=2, 3 and 5 for 4 hours. Additionally, the samples were contacted with a 100 mg/L solution of oxalic acid at pH=3, a typical reaction intermediate, that might cause Fe leaching through complexation [36]. The obtained results are presented in Table 4. Indeed, the presence of oxalic acid promotes the leaching of Fe, as observed by others [36].

Iron catalysts seem to be stable at pH values above 3; the Fe leached is lower than the limit of detection of employed analytical technique (0.03 mg/L). Copper dissolution is higher than iron dissolution over the whole pH range studied.

3.2. Fenton-like oxidation of phenol with D sample

3.2.1 Preliminary experiments

3.2.1.1. *Thermal decomposition.* Thermal decomposition of phenol was evaluated at 70°C in a five hour test. The phenol and TOC conversions were found to be negligible (3.5 %).

Phenol was also treated at 70°C in the absence of the catalyst using the stoichiometric amount of H₂O₂. Phenol and TOC reduction of 4 % was measured after 5 hours and pH value decreased from 4.7 to 4 at the end of the test.

3.2.1.2. *Phenol adsorption.* A mass of D equivalent to 100 mg/L of Fe in the reaction media was employed (0.57 g). Phenol and TOC conversions obtained (4-5 %) were similar to the values achieved during thermal decomposition.

3.2.2. Phenol oxidation tests

Preliminary experiments with D catalyst were executed varying initial pH value, particle size, catalyst loading and reaction temperature.

3.2.2.1. *Initial pH value and temperature effect.* Phenol oxidation was performed at 60 and 70°C with a loading of 0.57 g. The initial pH=3 was fixed with H₂SO₄ (2 mol/L), while the pH of the initial phenol solution was around 5. Experimental outcomes are presented in Fig. 10. Better results were obtained at pH=3. The pH value controls the generation rate of HO[•], the catalytic activity is usually high in the acidic medium and an optimum at around pH=3 is often reported [6, 37-42]. Furthermore, in heterogeneous systems where the oxidant adsorption is a rate-determining step, lower pH values promote H₂O₂ adsorption since the surface charge becomes more positive and H₂O₂ is a typical electron donor [40, 43].

At higher pH values, the oxidation potential of HO^\bullet decreases and the decomposition of H_2O_2 into O_2 and H_2O is accelerated. On the other hand, at lower pH values ($\text{pH} < 3.0$) hydrogen peroxide forms a stable oxonium ion (e.g. H_3O_2^+) and the scavenging effect of the HO^\bullet by H^+ is enhanced [4, 44].

At most conditions, as shown in Fig. 10, the presence of a three step mechanism is detected: the first step consists of a lag phase that is followed by an increase of the reaction rate to finally reach a plateau. The induction period is only present at $\text{pH}=5.2$, and decreases at higher temperatures, 90-120 min at 60°C and 60-90 min at 70°C . If only heterogeneous catalysis is taken into account, the lag could be related to the presence of just Fe(III) species on the catalyst surface that should be reduced to Fe(II) by H_2O_2 [45]. This reaction is at least 3-orders of magnitude slower than the classical Fenton reaction [46]. As more Fe(II) is produced, the depletion of H_2O_2 accelerates. Some of the intermediates formed such as catechol and 1,4-hydroquinone can also reduce Fe(III) to Fe(II) [47], being this route much faster than the reduction of Fe(III) by H_2O_2 and accounts for the transition from the lag phase to the reaction phase (or second step) [48].

On the other hand, if homogeneous contribution is considered, the lag phase could be associated to the time needed to dissolve enough iron for the homogeneous Fenton reaction to take place. However, since the high initial pH value (5.2) does not promote Fe dissolution, the initial homogeneous contribution should be negligible. Meanwhile, at $\text{pH}=3$ the reaction starts immediately. At this pH some Fe could be removed from the solid, although the Fe leached in this experiment is below the detection limit (0.03 mg/L). Moreover, accordingly to Kuan et al. [2] the presence of even ppb of Fe in solution can start the peroxidation, but not at relevant rates. Therefore, at the lowest pH the leaching of iron at the beginning of the test could encourage the homogeneous reaction with the appearance of intermediates such as catechol and 1,4-hydroquinone. These compounds may in term reduce Fe(III) to Fe(II) at a much

higher rate.

Finally, at longer reaction times and for both pH values studied, changes in conversions become sluggish, probably due to an increase of the Fe(III)/Fe(II) ratio [47, 49]. On the other hand, the hydroquinone-like intermediates that enhance peroxide decomposition may be worn out and the remaining products could be of refractory nature.

At 70°C the catalyst leached a total of 5 mg/L of Fe with initial pH=3, and a total of 4.3 mg/L with initial pH=5.2. At 60°C the catalyst leached 6.1 mg/L of Fe with initial pH=3 and 2.3 mg/L with initial pH=5.2. In spite of the higher initial reaction rates and Fe leaching the final mineralization at initial pH 3 was still 50-55 %. Results are comparable to those obtained by other more sophisticated Fe-based catalyts in the literature (Table 1).

It is interesting to point out that in the absence of phenol at 70°C and neutral pH, the different catalyst samples did not promote the H₂O₂ decomposition (only 5-20 % conversion). Therefore, during phenol oxidation the consumption of the oxidant would be promoted by the pH drop and generation of hydroquinone-like intermediates. Decomposition of H₂O₂ was also evaluated in bidistilled water at 70°C and pH=3 (Fig. S9). The final conversion achieved was much higher (38 %) than at neutral pH. However, an induction period was still observed, which is probably related to the Fe(II)/Fe(III) ratio.

3.2.2.2. Particle size effect.

Internal diffusional restrictions could affect the reaction rate by decreasing the reactants transport or the transfer of leached iron, reducing the homogeneous contribution [20, 36, 47, 50]. Furthermore, radicals could be formed on the diatomite surface at an important rate, but could be immediately recombined or scavenged before becoming available due to these diffusional restrictions [36].

To assess the effect of internal transport, the catalyst was grinded. Results for different catalyst sizes (powder and 2.38-2.83 mm) are presented in Fig. 11. Powdered samples provide

higher TOC and peroxide conversions after the first 60-90 min. However, improvements obtained could be related to a much higher extent of leaching (12 mg/L). Anyway, the 60-90 min induction period still remained for powdered solids.

3.2.2.3. *Catalyst loading effect.* Phenol oxidation was performed at 70°C, without pH control, with a diatomite loading equivalent to 22, 100 and 250 mg/L of Fe in the reaction media, which is 0.126, 0.57 and 1.428 g, respectively (Fig. S10).

With a higher catalyst loading the concentration of active sites increases and the reaction rate is accelerated. However, the final mineralization remains below 65 %: 12.8 % for 0.126 g, 52.7 % for 0.57 g and 64.9 % for 1.428 g. Also, leaching of iron increases with the catalyst concentration: 1 mg/L (catalyst loading 0.126 g), 4.3 mg/L (0.57 g) and 6.3 mg/L (1.428 g).

3.2.2.4. *Homogeneous contribution.* To evaluate if leached Fe is active a set of experiments were designed with 0.57 g of D sample, at 70°C and initial pH 5. The catalyst samples were filtered at different times leaving the supernatant reacting at 70°C until the five hours were completed (Fig. 12).

The reaction seemed to move further during one more hour after the catalyst was filtered. The presence of either remnant radicals and/or “fresh radicals” generated by the reaction between leached Fe and peroxide in solution may impel the oxidation. Then, the consumption of radicals or complexation of Fe may slow down the reaction and a plateau is noticeable, especially for the oxidant conversion. The heterogeneous Fenton process is likely to start on the oxide surface by the catalytic decomposition of adsorbed H₂O₂ leading to HO• and HO₂• species, which will attack nearby oxidant or pollutant molecules, with reduction and release of surface Fe³⁺ as Fe²⁺, in which H₂O₂ plays the role of reductant. Once in solution, Fe²⁺ will react with the remaining H₂O₂ as in a conventional homogeneous reaction [41]. This would be a combination of heterogeneous and homogeneous processes.

3.3. Modified diatomites

In order to improve reaction outcomes, three samples were tested: Fe-D, H-Fe-D and Cu/Fe-D. Results are compared with the thermally treated catalyst D.

3.3.1. Fe-D and H-Fe-D samples

Samples were tested at 60 and 70°C with a catalyst loading equivalent to 100 mg/L of Fe in the reaction mixture. Figure 13 shows results obtained with the three Fe-based catalysts: D, Fe-D and H-Fe-D, at 60°C and initial pH 5.

The performance of the Fe-D sample was inferior showing much lower phenol, TOC and H₂O₂ conversions and consequently only a small decrease of the pH value. This could be related to its slightly lower BET surface area, to the blockage of diatomite natural catalytic sites or less dispersed active phase. Besides, the iron added to the sample resulted less active and more labile than the natural iron of the diatomite. At this temperature the Fe-D leached 3.4 mg/L of the cation, while D and H-Fe-D leached around 2 mg/L.

Performances of D and H-Fe-D catalysts were similar in terms of phenol conversion but the acidic sample presented smaller induction time and higher initial reaction rates. Final TOC and peroxide conversions were also slightly higher for the H-Fe-D sample. Results can be explained through the nature of the active sites observed in the H-Fe-D sample: during the first step of phenol oxidation, the Brönsted sites of the H-Fe-D catalyst could promote the hydroxylation of phenol and the generation of hydroquinone-like compounds responsible of autocatalysis [51-53]. Several literature reports suggest the participation of Brönsted acid sites in the hydroxylation of phenol [54]. Hydroxylation of phenol in the presence of solids containing acid sites occurs by an electrophilic aromatic substitution mechanism in the orto or para positions, activated by resonance of the OH- group of phenol by a hydroxonium cation formed in the reaction of H₂O₂ with the acid centers of the solid [52]. Redox catalysts and acid catalysts for the hydroxylation of phenol proceed through differing mechanistic pathways. The pathway over the redox catalysts is reliant on hydroxyl radical formation,

while the acid pathway relies on the stabilization of phenoxy intermediates [53]. Accordingly to Germain et al. [51] who studied the role of acidity in the catalytic hydroxylation of phenol with H_2O_2 , a redox mechanism involving the couple hydroquinone/*p*-benzoquinone is responsible of autocatalysis. However, in the absence of an acid catalyst, neither hydroquinone nor *p*-benzoquinone can initiate the hydroxylation of phenol. This implies that the redox agent must be protonated in order to be active. The decomposition of hydrogen peroxide is then attributed to the simultaneous presence of hydroquinone/*p*-benzoquinone couple and acid sites on the catalyst surface.

At 70°C, initial reaction rates were only slightly higher for the acid treated catalyst and a final TOC conversion around 50 % was obtained with all the samples (Fig. S11). The impregnated catalyst samples leached higher amounts of Fe: 4.3 mg/L (D), 8.8 mg/L (Fe-D) and 7 mg/L (H-Fe-D). Fig. 14 presents the progressive leaching of each sample at 70°C. The natural iron in the framework of diatomite (mostly nontronite) is more stable than the iron added, as observed by other authors in the case of iron substituted Fe-MCM-41 compared to iron loaded Fe/MCM-41 [55]. However, in spite of the higher leaching, the Fe-diatom catalyst presented larger induction period and lower conversions.

3.3.1.1. Adsorption of reaction intermediates.

Desorption tests were performed placing each used catalyst sample (D, Fe-D or H-Fe-D) in 200 mL of bidistilled water at pH 11.1 and 70°C. The used samples were filtered after a 5 hours test, performed with a catalyst load equivalent to 100 mg/L of Fe, at 70°C and initial pH 5. Samples were dried at room temperature before the desorption tests.

The pH value selected for the tests (pH 11) is much higher than the point of zero charge of the catalyst samples; therefore, a change of the catalyst surface charge from positive to negative is expected, which could cause the release of compounds adsorbed by electrostatic interactions [39]. The same test was also performed with a fresh catalyst sample. A total carbon (TC)

amount released of around 2 mg/L was measured in all cases (Table S4). This indicates that the amount of electrostatic adsorbed compounds is small in the given range of operating conditions studied.

In order to further evaluate the adsorption capacity of the catalyst samples, the adsorption of oxalic acid (50 mg/L, 70°C), a common reaction intermediate, was studied. No TOC reduction was observed after 4 hours.

3.3.1.2. Catalyst stability: D and H-Fe-D samples. In order to evaluate long-term stability of catalysts, a mass equivalent to 100 mg/L of Fe in the reaction mixture was retained and used again in successive runs at 70°C, without treatment of the catalyst samples between tests. The catalysts were used in four consecutive oxidation reactions of five hours each. The Fe-D sample was not evaluated taking into account its poorer performance and enhanced leaching.

Fig. 15 shows that both samples are still active after 20 hours of use. However, the impregnated acid catalyst leached more Fe, especially during the first cycle. The D and H-Fe-D samples leached a total of 12 and 24 % of the initial Fe content, respectively. As observed before, iron present in the impregnated samples is more labile.

Metal leaching is hard to avoid during the heterogeneous Fenton oxidation of organic pollutants. In order to remove the metal leached, the heterogeneous Fenton process could be coupled with a precipitation or filtration step [56, 57] which would generate a reduced volumen of sludge in comparison with a homogeneous process.

3.3.2. Cu/Fe-diatom sample

The Cu/Fe-D sample was tested at 70°C using a catalyst loading equivalent to 100 mg/L of Cu and 164 mg/L of Fe in the reaction suspension. Results are compared with outcomes obtained with D sample in Fig.16. Remarkably, initial reaction rates were considerably higher and no induction period was observed. The pH sharply decreased and then increased, indicating the

formation of acids and their subsequent mineralization. In agreement to these trends, a final mineralization of 86 % was obtained.

The absence of induction period can be explained by a somewhat different mechanism of radicals generation and phenol oxidation for Cu-containing systems [19, 58]. The mineralization level was remarkably higher; therefore, reaction intermediates which are refractory for Fe catalysts, may represent no challenge for copper-based catalysts [20]. It appears that Cu^{2+} complexes with organic acids are easily decomposed by HO^\bullet , whereas the corresponding Fe^{3+} complexes are highly stable; as a result, unlike Fe^{3+} -based systems, Cu^{2+} complexation does not block (or deactivate) the Fenton reaction or prevent near complete mineralization of organic pollutants [46].

So far, the bimetallic catalyst significantly surpasses all the Fe-based performances. However, leaching was excessive (12.7 mg/L of Cu and 3.8 mg/L of Fe). Further examination and characterization of this material was dismissed at the present time due to the high toxicity of copper [58].

4. Conclusions

Diatomite samples were modified by acid or base treatments, addition of Fe or Cu through the IWI method and calcination at 700°C. According to our characterization raw diatomite is a composite material consisting mostly of a clay structure (albite, nontronite) in which the frustules (albite and quartz) are included. Iron is present mostly as Fe(III) in cis octahedral sites, as observed by Mossbauer.

Contrary to the results obtained by other authors the base activation caused a decrease of BET surface area and pore volume probably due to the formation of a sodium silicate layer.

Acid treatment increased surface area and the amount of weak acid sites (Brönsted sites).

The Fe addition without any further treatment (Fe-D) caused a decrease of the surface area.

Cu addition (Cu/Fe-D) did not significantly change surface area, but CuO clusters were

identified. Acid treatment followed by Fe impregnation (H-Fe-D) showed best results in terms of surface area and amount of acid sites.

Modified diatomites were tested as catalysts for the Fenton-like oxidation of phenol at various operating conditions. The diatomite calcined at 700°C (D) achieved complete phenol removal and a final mineralization around 50 %, with an average leaching between 4-6 mg/L.

The Fe-D sample presented a poor performance, which could be related to a slightly lower surface area, blockage of diatomite natural catalytic sites or less disperse active phase. Besides, the iron added to the sample resulted less active than the natural iron of the diatomite.

The acidic treatment favored the initiation of the reaction. The Brönsted sites could promote the hydroxylation of phenol and generation of the hydroquinone-like compounds responsible of autocatalysis (Kurian and Sugunan 2006).

The D and H-Fe-D samples were used in consecutive runs (up to 20 h) maintaining the performance in terms of phenol conversion and TOC reduction. After 20 hours of usage the H-Fe-D sample leached twice the iron leached by D (12%).

The Cu/Fe-D sample presented a mineralization level remarkably high (86%). However, leaching was excessive, 12.7 mg/L of copper and 3.8 mg/L of Fe.

Homogeneous contribution was evaluated for the calcined sample (D). Iron is leached progressively and its contribution to the oxidation reaction cannot be discarded. Fe leached deactivates due to complexation and as it was observed in the case of the Fe-D sample, higher leaching does not move further the oxidation reaction.

Overall, these modified natural catalysts presented a good performance, even comparable to more sophisticated materials

Acknowledgements - Financial support from CONICET, UNMdP, ANPCyT (Argentina) and Fundación Carolina (España). We also want to express our gratitude to C. Rodriguez, J. Cechini and H. Asencio for their technical support. This research was partly supported by the Spanish Ministerio de Educación y Ciencia and FEDER, project CTM2011-23069. Dr. Font is part of a research group recognized by the Comissionat per a Universitats i Recerca del DIUE de la Generalitat de Catalunya (2014 SGR 1065) and supported by the Universitat Rovira i Virgili (2010PFR-URV-B2-41).

References

- [1] K. Barbusinski, *Ecol. Chem. Eng. S.* 3(16) (2009).
- [2] C.C. Kuan, S.Y. Chang, S.L.M. Schroeder, *Ind. Eng. Chem. Res.* 54(33) (2015) 8122-8129.
- [3] R.M. Liou, S.H. Chen, M.Y. Hung, C.S. Hsu, J.Y. Lai, *Chemosphere* 59 (2005) 117-125.
- [4] J. Guo, M. Al-Dahhan, *Eng. Chem. Res.* 42 (2003) 2450-2460.
- [5] F. Martínez, J.A. Melero, J.A. Botas, M.I. Pariente, R. Molina, *Ind. Eng. Chem. Res.* 46 (2007) 4396-4405.
- [6] C.B. Molina, J.A. Casas, J.A. Zazo, J.J. Rodríguez, *Chem. Eng. J.* 118 (2006) 29-35.
- [7] P. Bautista, A.F. Mohedano, J.a. Casas, J.a. Zazo, J.J. Rodríguez, *J. Chem. Technol. Biotechnol.* 86(4) (2011) 497-504.
- [8] O.P. Pestunova, O.L. Ogorodnikova, V.N. Parmon, *Chem. Sustain. Dev.* 11 (2003) 227-232.
- [9] C. di Luca, F. Ivorra, P. Massa, R. Fenoglio, *Chem. Eng. J.* 268 (2015) 280-289.
- [10] M. Xia, M. Long, Y. Yang, C. Chen, W. Cai, B. Zhou, *Appl. Catal. B: Environ.* 110 (2011) 118-125.
- [11] E. Garrido-Ramírez, B.K.G. Theng, M.L. Mora, *Appl. Clay Sci.* 47(3-4) (2010) 182-192.
- [12] C.B. Molina, J.A. Casas, A.H. Pizarro, J.J. Rodríguez, in: J.P. Humphrey and D. E. Boyd (Eds). *Pillared Clays as Green Chemistry Catalysts: Application to Wastewater Treatment*. Nova Science Publishers, Inc. 2011. pp. 435-474.
- [13] N. Inchaurredo, J. Font, C.P. Ramos, P. Haure, *Appl. Catal. B: Environ.* 181 (2016) 481-494.
- [14] H. Valdés, V.J. Farfán, J.A. Manolí, C.A. Zaror, *J. Hazard. Mater.* 165 (2009) 915-922.

- [15] X. Liu, C. Yang, Y. Wang, Y. Guo, Y. Guo, Gu. Lu, *Chem. Eng. J.* 243 (2014) 192-196.
- [16] W.T. Tsai, K.J. Hsien, C.W. Lai, *Ind. Eng. Chem. Res.* 43 (2004) 7513-7520.
- [17] Z. Jian, P. Qingwei, N. Meihong, S. Haiqiang, L. Na, *Appl. Clay Sci.* 83–84 (2013) 12-16.
- [18] M. Aivalioti, P. Papoulias, A. Kousaiti, E. Gidarakos, *J. Hazard. Mat.* 207–208 (2012) 117-127.
- [19] M.N. Timofeeva, S.Ts. Khankhasaeva, E.P. Talsi, V.N. Panchenko, A.V. Golovin, E.Ts. Dashinamzhilova, S.V. Tsybulya, *Appl. Catal. B: Environ.* 90 (2009) 618-627.
- [20] J. Maekawa, K. Mae, H. Nakagawa, *J. Environ. Chem Eng.* 2 (2014) 1275-1280.
- [21] A. Chaisena, K. Rangriwatananon, J. Suranaree, *Sci. Technol.* 11 (2004) 289-299.
- [22] M.a.M. Khraisheh, M.a. Al-Ghouti, S.J. Allen, M.N. Ahmad, *Water Res.* 39(5) (2005) 922-932.
- [23] G.K. Pedersen, S.A.S. Pedersen, J. Steffensen, C.S. Pedersen, *Bulletin of the geological society of Denmark* 51 (2007) 159-177.
- [24] T. Preočanin, N. Kallay, *Croat. Chem. Acta.* 71(4) (1998) 1117-1125.
- [25] L.S. Clesceri, in: L.S. Clesceri, A.E. Greenberg, A.D. Eaton (Eds.). *Standard Methods for the Examination of Water and Wastewater*. 20th ed., American Public Health Association, Washington, DC, 1998.
- [26] D. Gaoxiang, L. Guocheng, H. Xuwen, *Chinese J. Chem. Eng.* 21(7) (2013) 736-741.
- [27] B. A. Goodman, J. D. Russell, A. R. Fraser and F. W. D. Woodhams, *Clay. Clay Miner.* 24 (1976) 53-59.
- [28] I. Rozenson, L. Heller-Kallai, *Clay. Clay Miner.* 25 (1977) 94-101.
- [29] J. M. D. Coey, *Atom. Energy Rev.* 18 (1980) 73-124.
- [30] L. Heller-Kallai, I. Rosenson, *Phys. Chem. Minerals* 7 (1981) 223-238.
- [31] D. Bonnin, G. Calas, H. Suquet, H. Pezerat, *Phys. Citem. Minerals* 12 (1985) 55-64.
- [32] A. Decarreau, F. Colin, A. Herbillon, A. Manceau, D. Nahon, H. Paquet, D. Trauth-Badaud, J. J. Trescases, *Clay. Clay Miner.* 35 (1) (1987) 1-10.

- [33] A. Manceau, V.A. Drits, B. Lanson, D. Chateigner, J. Wu, D. Huo, W.P. Gates, J.W. Stucki, *Amer. Miner.* 85 (2000) 153.
- [34] M.A. Al-Ghouti, M.A.M. Khraisheh, S.J. Allen, M.N. Ahmad, *J. Environ. Manage.* 69 (2003) 229-238.
- [35] S.V. Sirotin, I.F. Moskovskaya, B.V. Romanovsky, *Catal. Sci. Technol.* 1 (2011) 971-980.
- [36] B. Ortiz de la Plata, O. M. Alfano, A. E. Cassano, *Appl. Catal. B: Environ* 95 (2010) 1-13.
- [37] N. Crowther and F. Larachi, *Appl. Catal. B* 46 (2003) 293-305.
- [38] J.M. Tatibouët, E. Guélou, J. Fournier, *Top. Catal.* 33 (2005) 225-232.
- [39] J.A. Zazo, J.A. Casas, A.F. Mohedano, J.J. Rodríguez, *Appl. Catal. B: Environ.* 65 (2006) 261-268.
- [40] R. Andreozzi, M. Canterino, V. Caprio, I. Di Somma, R. Marotta, *J. Hazard. Mater.* 152 (2008) 870-875.
- [41] F.V.F. Araujo, L. Yokoyama, L.A.C. Teixeira, J.C. Campos, *Braz. J. Chem. Eng.* 28(4) (2011) 605-616.
- [42] M. Muñoz, Z.M. de Pedro, N. Menendez, J.A. Casas, J.J. Rodriguez, *Appl. Catal. B: Environ.* 136-137 (2013) 218-224.
- [43] X. Huang, J. Ding, Q. Zhong, *Appl. Surf. Sci.* 326 (2015) 66-72.
- [44] S.H. Tian, Y.T. Tu, D.S. Chen, X. Chen, Y. Xiong, *Chem. Eng. J.* 169(1-3) (2011) 31-37.
- [45] J.J. Pignatello, E. Oliveros, A. MacKay, *Critical Reviews in Environmental Science and Technology* 36:1 (2006) 1-84.
- [46] A.D. Bokare, W. Choi, *J. Hazard. Mater.* 30 (2014) 121-135.
- [47] Y. Du, M. Zhou, L. Lei, *J. Hazard. Mater.* 136(3) (2006) 859-865.
- [48] R. Chen and J. J. Pignatello, *Environ. Sci. Technol.* 31 (1997) 2399-2406.
- [49] C. Jiang, S. Pang, F. Ouyang, J. Mac, J. Jiang, *Journal of Hazardous Materials* 174 (2010) 813-817.
- [50] L. Xu, J. Wang, *J. Hazard. Mater.* 186 (2011) 256-264.
- [51] A. Germain, M. Allian, F. Figueras, *Catal. Today* 32 (1996) 145-148.

- [52] S. Letaïef, B. Casal, P. Aranda, M. A. Martín-Luengo, E. Ruiz-Hitzky, *Appl. Clay Sci.* 22 (2003) 263-277.
- [53] J. Pui Ho Li, E. Kennedy, M. Stockenhuber, *Catal. Lett.* (2014) 144:9-15
- [54] M. Kurian and S. Sugunan, *Chem. Eng. J.* 115 (2006) 139-146.
- [55] B. Lan, R. Huang, L. Li, H. Yan, G. Liao, X. Wang, Q. Zhang, *Chem. Eng. J.* 219 (2013) 346-354.
- [56] N. Inchaurredo, E. Contreras, P. Haure, *Chem. Eng. J.* 251 (2014) 146-157.
- [57] N. Inchaurredo, P. Haure, J. Font, *Desalination* 315 (2013) 76-82.
- [58] WHO. Copper in drinking-water background document for development of WHO guidelines for drinking-water quality. in: World Health Organization. 2004.

Table 1. Fe-based catalysts for the peroxidation of concentrated phenol solutions.

Catalyst	Phenol conversion (%)	TOC conversion (%)	pH	Operating conditions	Leaching	Ref.
Fe(III) -M1 resin	10, 100, 100 (40, 60, 80°C)	23, 79, 75 (COD) (40, 60, 80°C)	Not controlled	Phenol 1000 mg/L, H ₂ O ₂ 0.1 mol/L, 5 g/L catalyst, 40, 60, 80°C, 2 hours, 25 mg Fe/g resin	Not reported	[3]
Pillared clays Al-Fe	100	45	Initial pH 4	Phenol 500 mg/L, H ₂ O ₂ 0.3 mol/L, continuous feed 0.21-0.84 mol/min, 6.6 g/L catalyst, 4 hours, 50°C, 7.02 % wt/wt of Fe ₂ O ₃	<0.4 mg/L	[4]
Fe ₂ O ₃ /SBA-15	100	66	Not controlled	Phenol 1000 mg/L, H ₂ O ₂ stoichiometric, 2.9 g catalyst, residence time 3.8 min, 80°C, 14 % of Fe	1.3 % after 34 hours	[5]
Pillared clays Al/Fe y Zr/Fe	100	65 (Al/Fe-PC) 50 (Zr/Fe-PC)	pH 3-3.5	Phenol 2000 mg/L, H ₂ O ₂ stoichiometric, 6.6 g/L catalyst, 6 hours, 25°C, 1.11 mmol Fe/g clay	Al/Fe: 2 mg/L (1 %) Al/Zr: 5 mg/L (2 %)	[6]
Fe- γ Al ₂ O ₃	100	49	3	Phenol 1000 mg/L, H ₂ O ₂ stoichiometric, 1250 mg/L catalyst, 8 hours, 50°C, 4 % wt/wt of Fe	5.3 mg/L	[7]
Fe- α Al ₂ O ₃	100	26	Not controlled	Phenol 940 mg/L, 0.1 mol/L H ₂ O ₂ , 5 g/L catalyst, 3 hours, 90°C, 2 % wt/wt of Fe	21 %	[8]
Fe- γ Al ₂ O ₃ IC-12-74	100	56	Not controlled	Phenol 940 mg/L, 0.1 mol/L H ₂ O ₂ , 5 g/L catalyst, 3 hours, 90°C, 4 % wt/wt of Fe	5 %	[8]
Fe- γ Al ₂ O ₃	100	63	Not controlled	Phenol 5000 mg/L, H ₂ O ₂ :phenol molar ratio 11.2, 7.2 g/L catalyst, 4 hours, 70°C, 0.53 % wt/wt Fe	30 %	[9]
Fe-MCM-41 (M2)		12	4	Phenol 200 mg/L, H ₂ O ₂ 0.049 mol/L, 1.5 g/L catalyst, 2 hours, 40°C, 2.55 % wt/wt Fe		[10]
D	100	53	Not controlled	Phenol 1000 mg/L, H ₂ O ₂ 1.3 stoichiometric, 2.85 g/L catalyst, 5 hours, 70°C, 3.4 % wt/wt Fe	4.3 mg/L	This study

Table 2. Catalyst characterization, BET surface area, active metal content and EDX composition.

Sample	S_{BET} (m^2/g)	V_{pore} (cm^3/g)	d_{pore} (nm)	Fe or Cu (%)	Fe or Cu EDX content (wt. %)	
					Core	Surface
Raw	132.5	0.26	7.9	3	3.85±1	3.9±1.3
D	82.7	0.28	10	3.5	2.3	4.1±1.1
HNO ₃ /raw sample	157.3	0.3	9.6	3	5.4±0.2	5±1.3
Na-Fe-D	45	0.1	1.9	6.84	3.6	11.7
H-Fe-D	85.1	0.27	10.9	5.33	9.7±1.3	12.1±5
Cu/Fe-D	77.4	0.27	10.7	2.05 Cu and 3.4 Fe	2.2 Cu	1.8±0.5 Cu
Fe-D	56.7	0.19	10.8	5.4	5.6±0.3	8±2
Used H-Fe-D	126.9	0.31	9.9	4.1	9±4	6±1
Used D	141.1	0.33	9.5	3.1	5.2±3.8	3±1

Table 3. Acid sites in diatomite samples.

Sample	Acid sites density (mmol/m ²)	Acid sites quantity (mmol/g)	Pyridine desorption temperature (°C)
D	6.56×10^{-4}	0.054	238, 630
H-Fe-D	7.39×10^{-4}	0.063	233, 335, 556
Fe-D	8.64×10^{-4}	0.049	228, 523

Table 4. Iron leached during stability tests conducted at room temperature.

Catalyst sample	Iron leached (mg/L)			
	pH=2	pH=3	pH=5	Oxalic acid
D	1.3	negligible	negligible	0.4
Fe-D	1.1	negligible	negligible	0.9
H-Fe-D	0.85	negligible	negligible	0.7
Cu/Fe-D	7 (Cu)	1.4 (Cu)	negligible	2.4 (Cu)

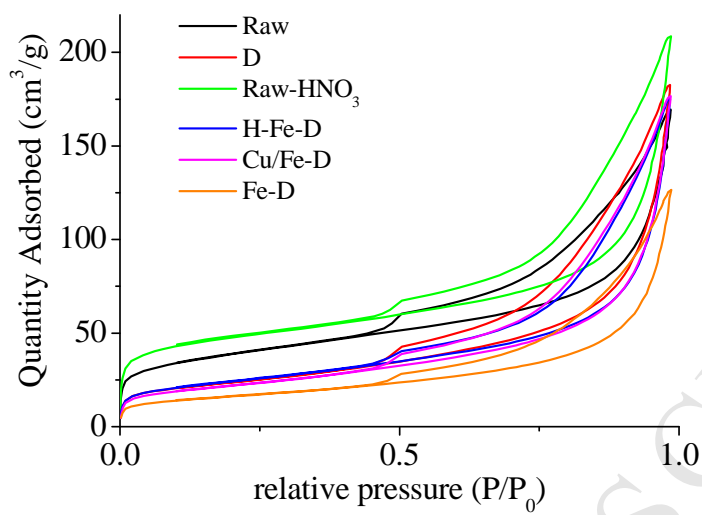


Fig. 1. N₂ adsorption-desorption isotherms of selected samples.

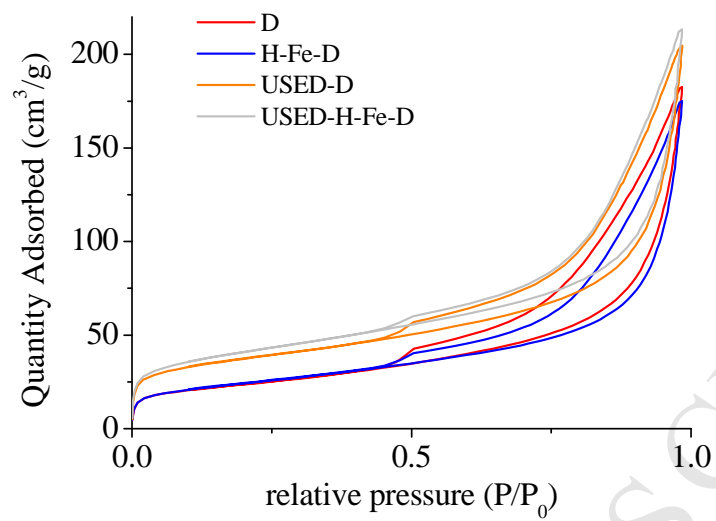


Fig. 2. N₂ adsorption-desorption isotherms of selected samples.

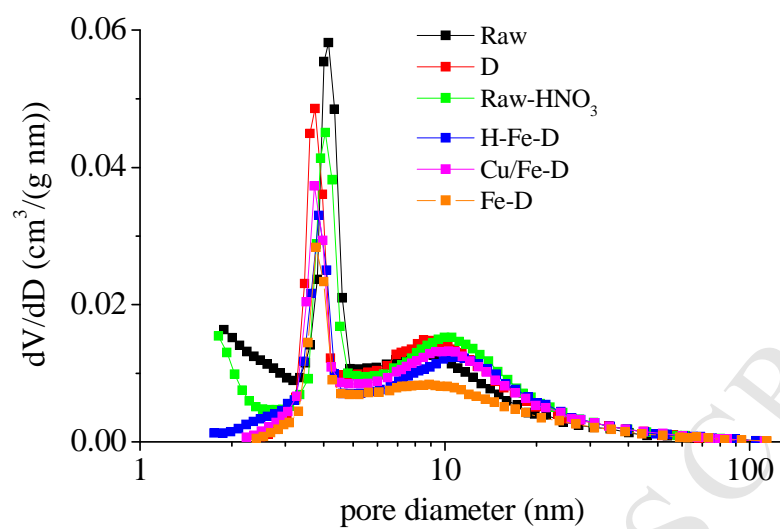


Fig. 3. BJH pore size distribution of selected samples.

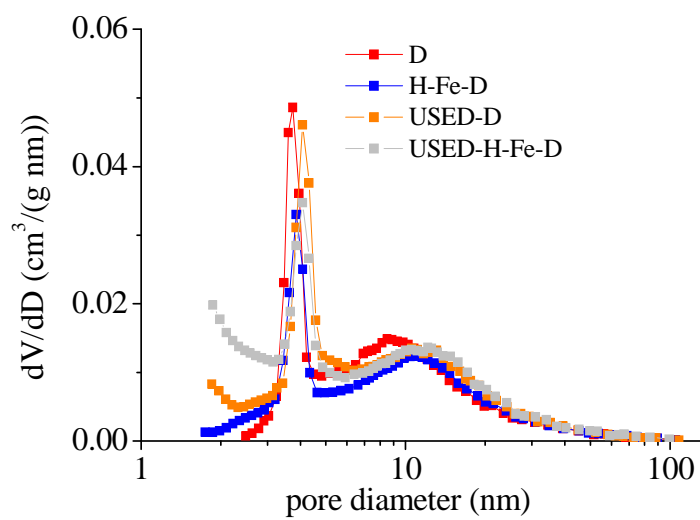


Fig. 4. BJH pore size distribution of selected samples.

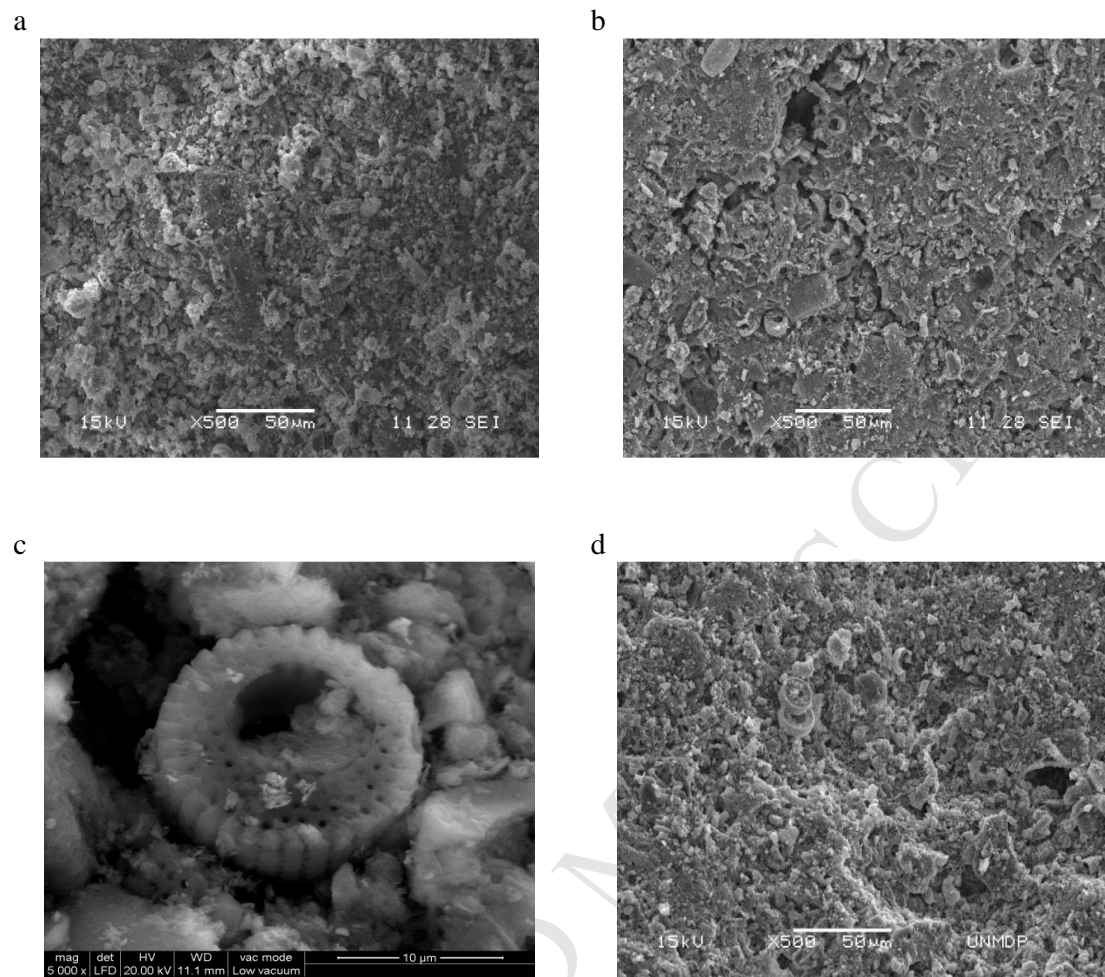


Fig. 5. SEM images of a) Raw, b) Base activated, c) Fe-D and d) H-Fe-D

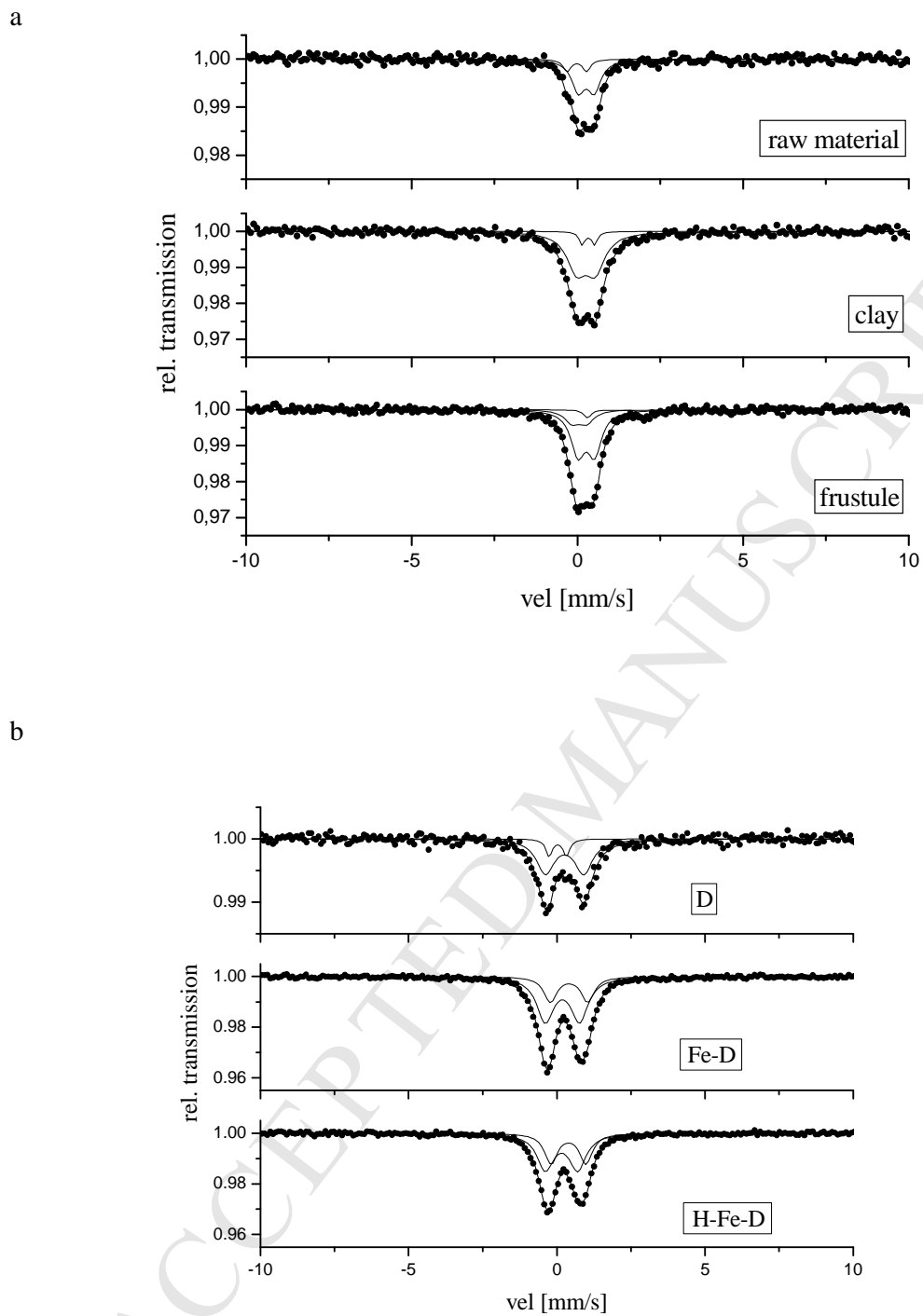


Fig. 6. Mössbauer spectra of: a) raw material, clay and frustule; b) D, Fe-D and H-Fe-D

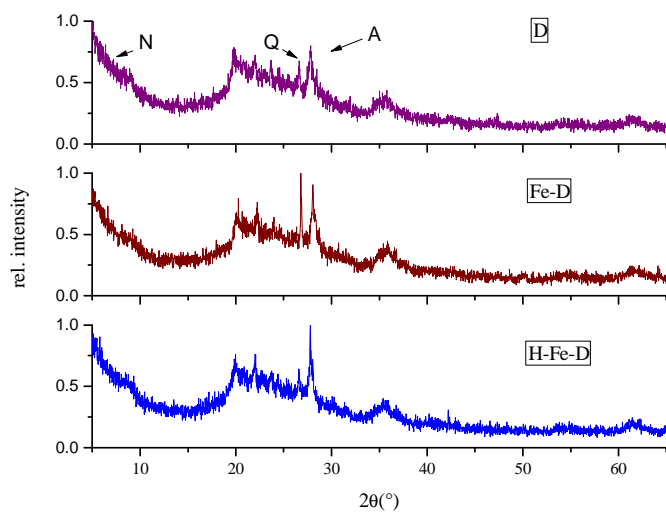


Fig. 7. XRD diffractograms of: a) raw material, clay and frustule; b) D, Fe-D and H-Fe-D samples. A: albite, N: nontronite, Q: quartz.

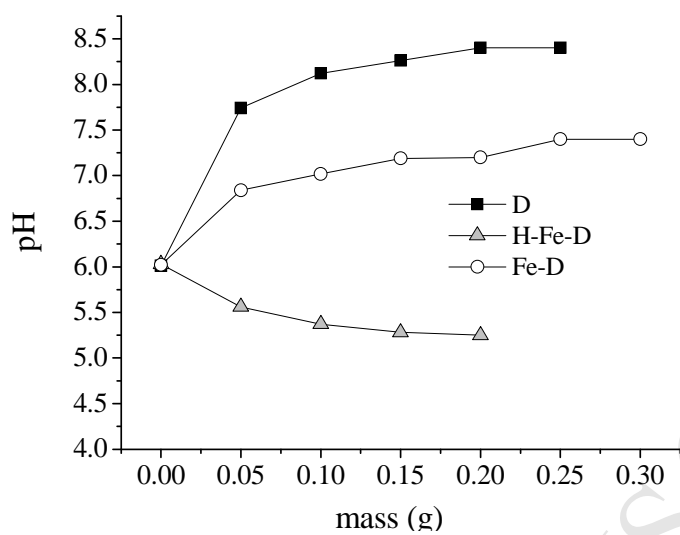


Fig. 8. Mass titration curves for catalyst samples in 0.005 mol/L NaCl.

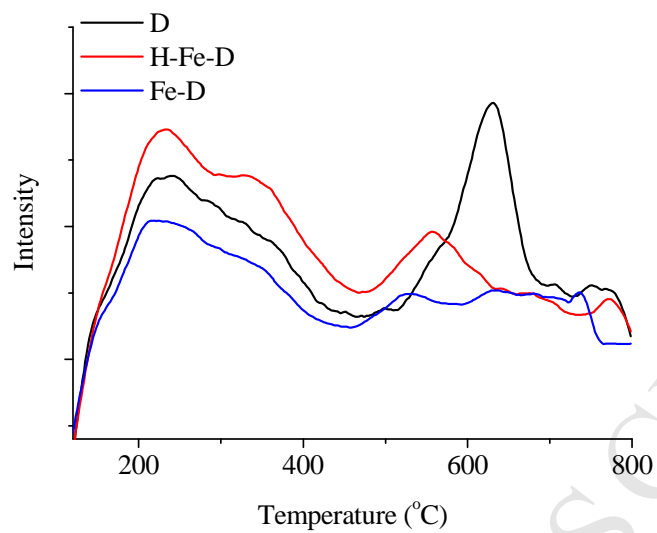


Fig. 9. Pyridine TPD curves for tested catalyst samples.

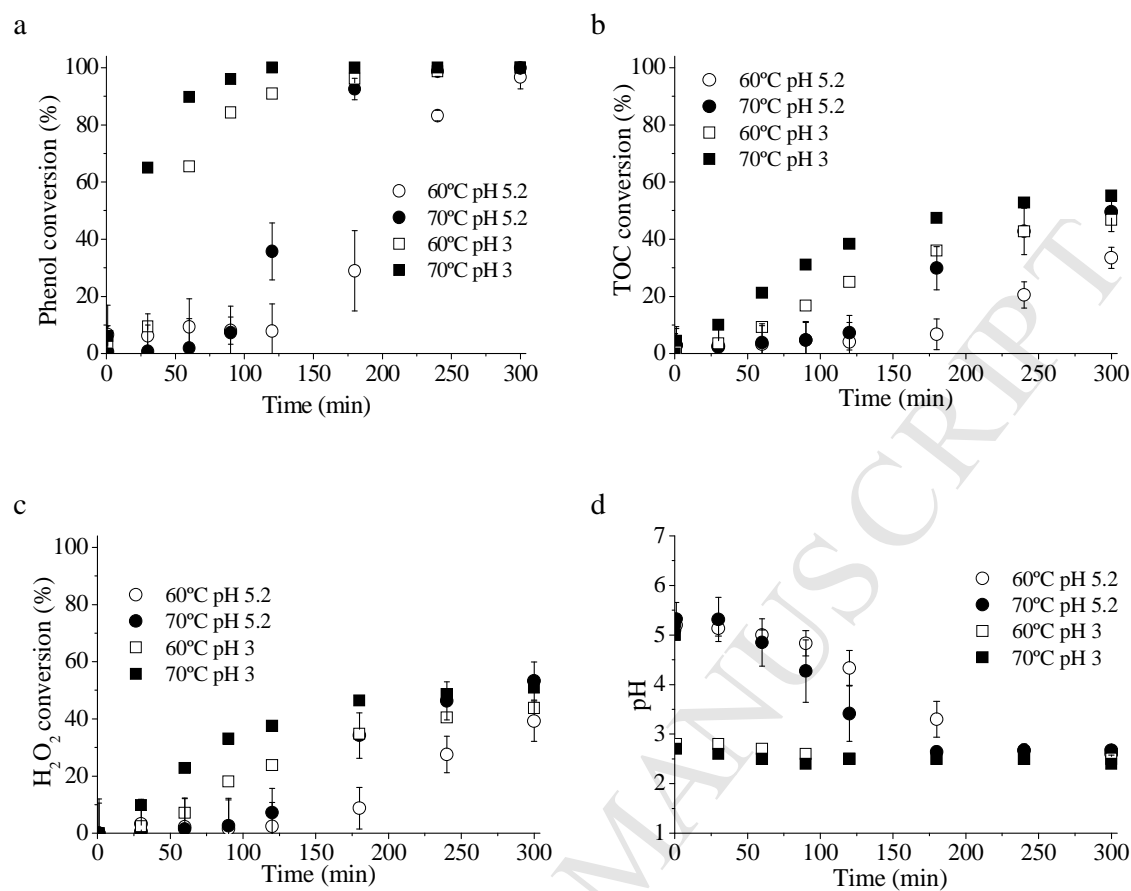


Fig. 10. Conversion of a) phenol, b) TOC, c) H₂O₂ and d) pH evolution as a function of time over D sample at 60 and 70°C and initial pH values (3 or 5.2).

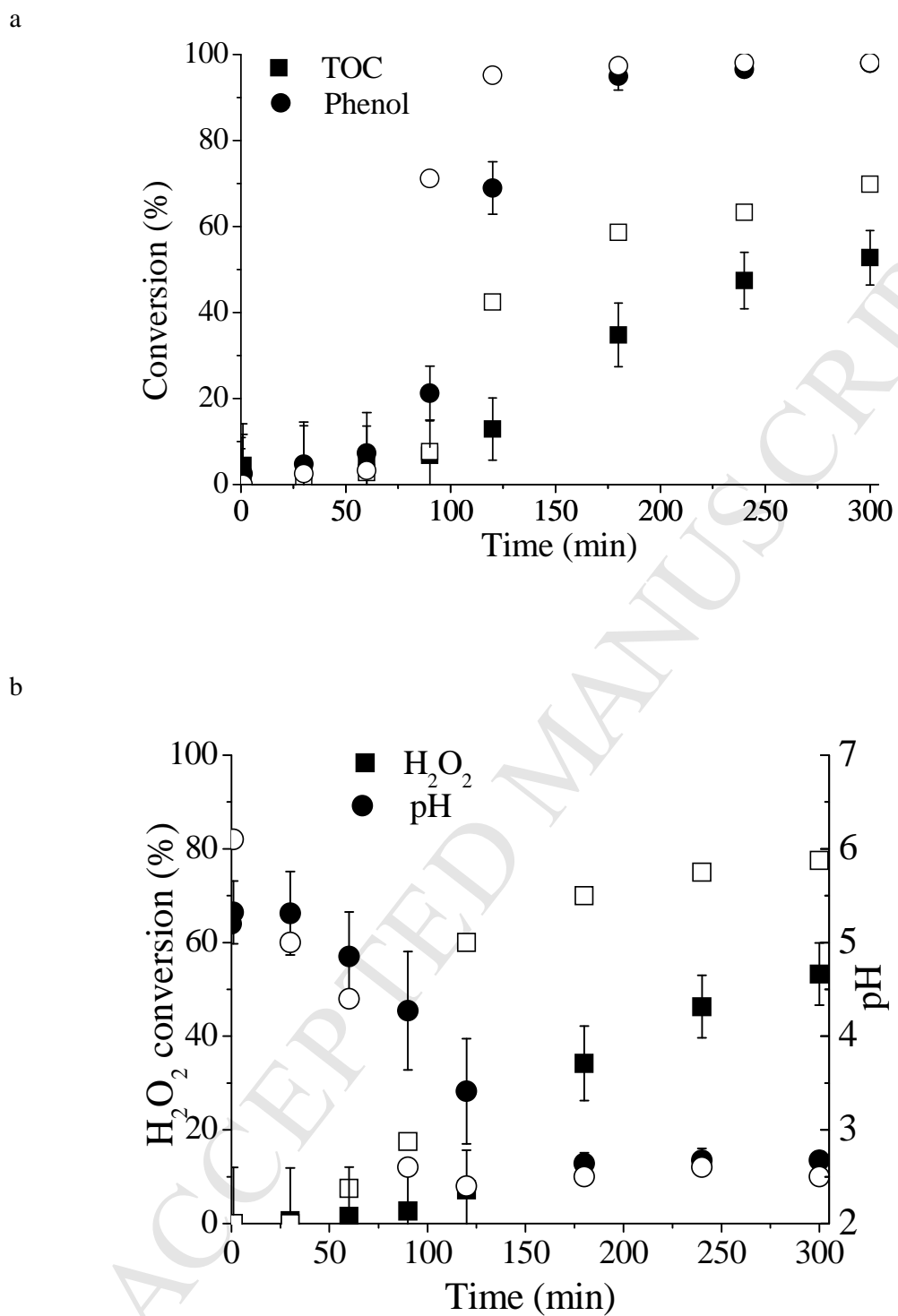


Fig. 11. a(a) Phenol and TOC conversions over time, (b) H₂O₂ conversion and pH evolution over time, with particle catalyst (full symbol) and powdered catalyst (empty symbol).

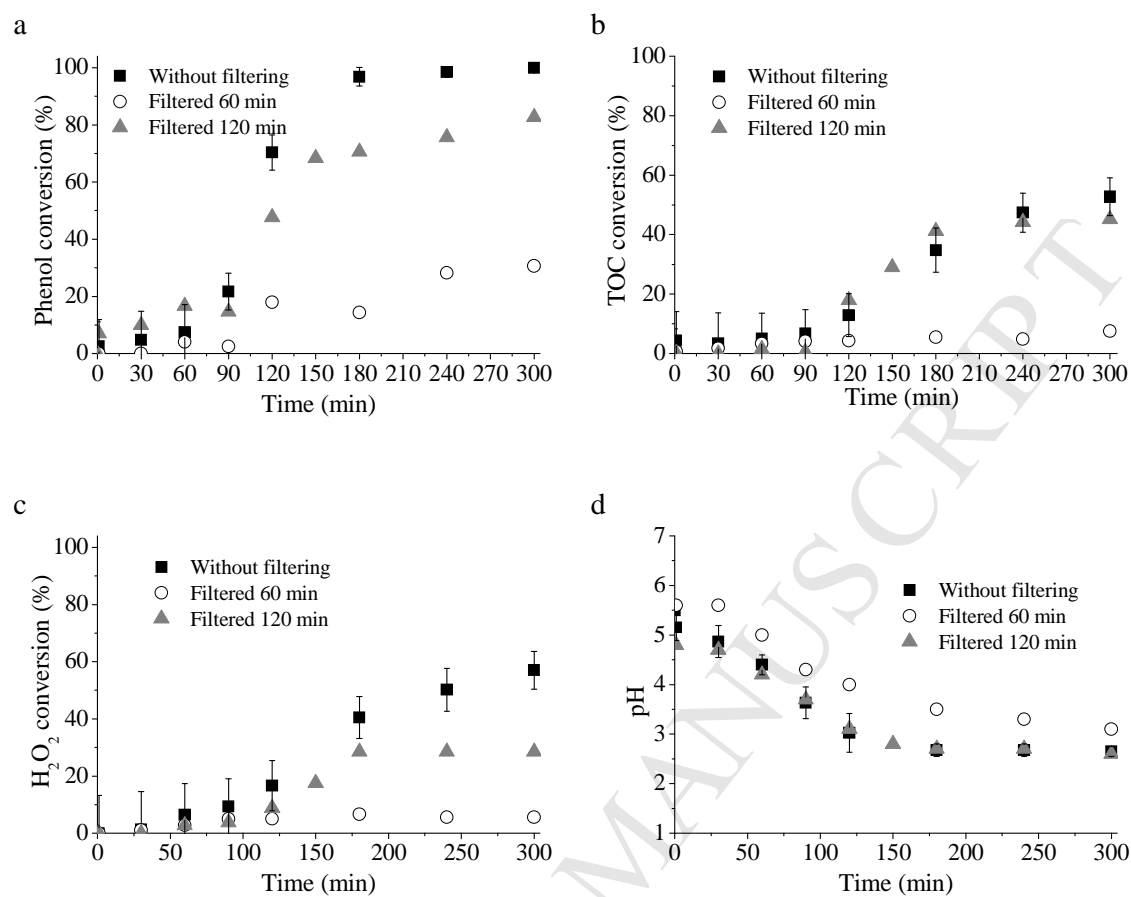


Fig. 12. Conversion of a) phenol, b) TOC, c) H₂O₂ and d) pH evolution as a function of time over D sample. Filtration of the catalyst at different times (60, 120 min and no filtering).

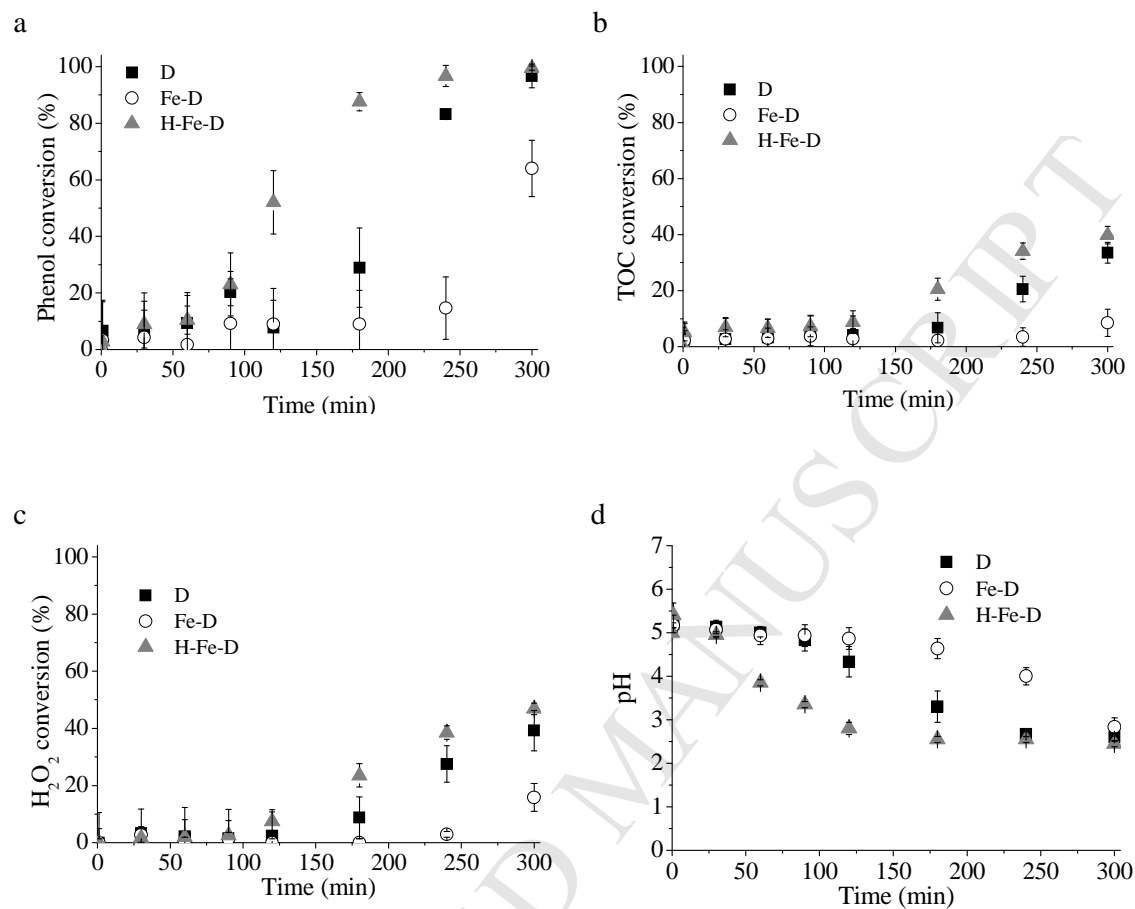


Fig. 13. Conversion of a) phenol, b) TOC, c) H₂O₂ and d) pH evolution as a function of time for different catalysts at 60°C. Catalyst loading equivalent to 100 mg/L of Fe in the reaction mixture.

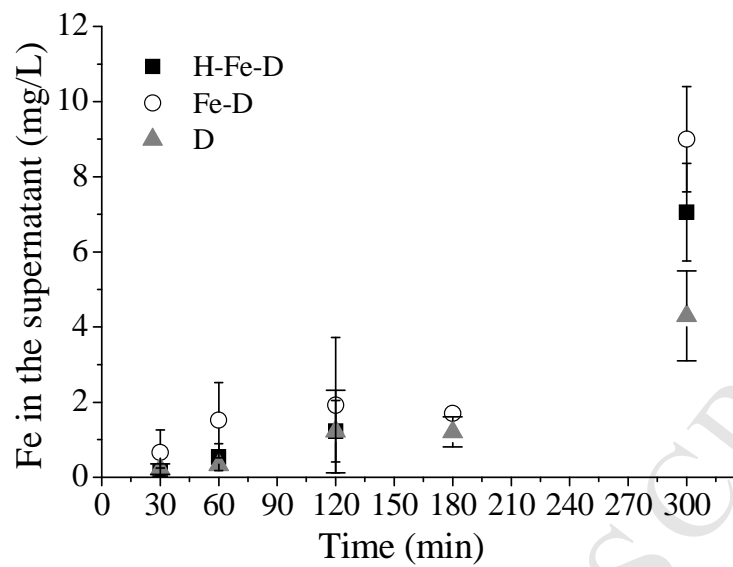


Fig. 14. Progressive leaching along the reaction time.

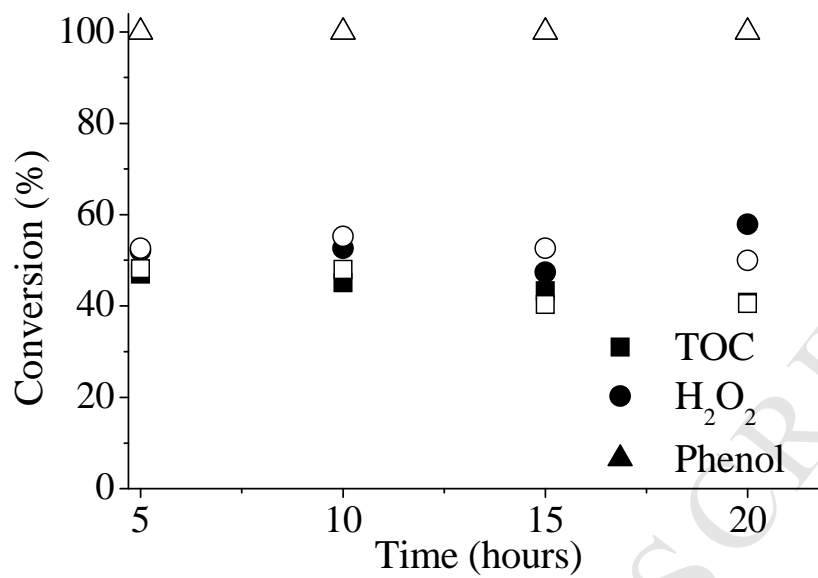


Fig. 15. Final conversions of phenol (circle), TOC (square) and H₂O₂ (triangle) after each five hours test for different catalyst samples: D (empty symbol), H-Fe-D (full symbol).

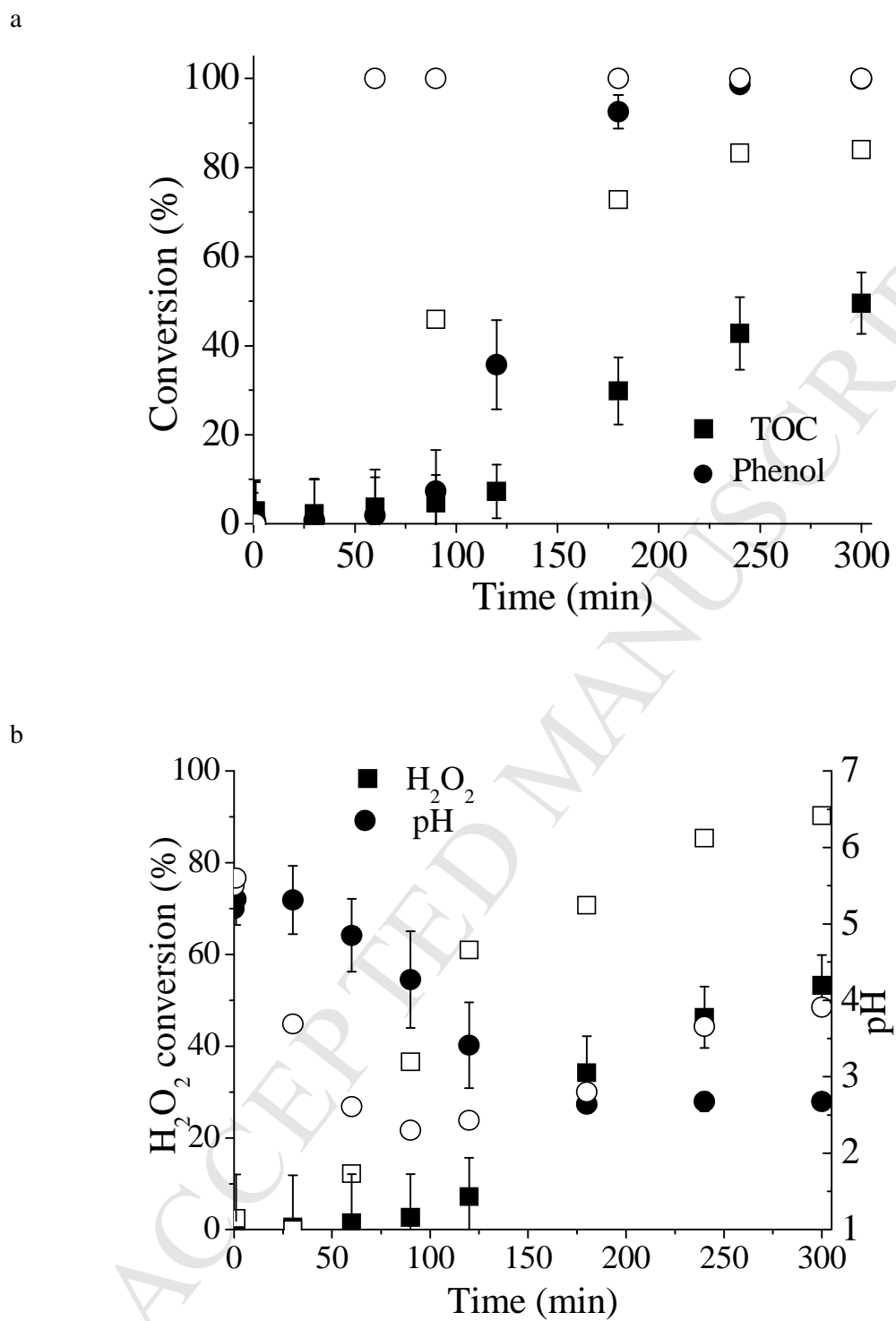


Fig. 16. a) Phenol and TOC conversions over time, b) H₂O₂ conversion and pH evolution over time using D (full symbol) and Cu/Fe-D (empty symbol) samples.

- Modified diatomite as a catalyst for Fenton-like oxidation of phenol.
- Acid activation of the material enhances phenol oxidation.
- At 70°C, iron catalysts achieve complete phenol removal and 50-55 % TOC reduction.
- Copper diatomite catalyst allows remarkably high TOC conversions (80 %).
- Iron diatomite catalysts used in consecutive runs yield similar performance.